

Mantle plume tomography

Guust Nolet^a, Richard Allen^b, Dapeng Zhao^{c,*}

^a *Department of Geosciences, Princeton University, Princeton, NJ 08544, United States*

^b *Department of Earth and Planetary Science, University of California, Berkeley, CA 94720, United States*

^c *Geodynamics Research Center, Ehime University, Matsuyama 790–8577, Japan*

Accepted 22 January 2007

Abstract

We review the resolution currently available with seismic tomography, in particular the ability of seismic waves to image mantle plumes, and discuss frequently asked questions about artifacts, interpretation and possible systematic errors. These aspects are discussed in more detail for two case histories offering different problems in the tomographic interpretation: Iceland and Hawaii. Regional and global models resolve a vertical low velocity anomaly beneath Iceland, interpreted as an upwelling, from the transition zone up to the base of the lithosphere. Beneath the transition zone any continuation of the low-velocity anomaly is weak at best. This may be due to the absence of such an anomaly, poor seismic resolution in the lower mantle, or the weak sensitivity of velocity to buoyancy at these depths. While we are confident of the presence of a plume in the upper mantle, its origins remain to be resolved. Because of its large distance to most seismic sources and stations, the mantle structure under Hawaii is among the most difficult to image tomographically, but several recent global tomography studies agree on a whole-mantle plume under the Hawaiian hotspot. The plume exhibits a tilting geometry, which is likely due to the mantle flow. Theoretical advances, as well as deployments of large seismic networks across hotspot regions, are expected to bring significant improvements to the imaging of narrow mantle upwellings in the near future.

© 2007 Elsevier B.V. All rights reserved.

Keywords: Seismic tomography; Mantle plumes; Upper mantle; Lower mantle

1. Introduction

Seismologists have known for a long time how to interpret the arrival times of seismic waves to determine the time and location of earthquakes as well as the variation of seismic wavespeed with depth. In the 20th century, such layered Earth models were subject to ever increasing refinements until it became evident that a

simple depth-dependence of seismic velocities was insufficient to explain the remaining discrepancies between observed and predicted arrival times. In the footsteps of medical tomography, where radiologists began to use computers to obtain X ray scans that focus on a plane of interest, two pioneering groups at MIT and Harvard obtained the first seismological tomograms of the Earth's interior by mapping anomalies in the compressional seismic velocity V_p (Aki and Lee, 1976; Dziewonski et al., 1977).

Whereas a medical CAT-scan is obtained by illuminating the body from all angles, the seismological scan is much more primitive: it is constructed from a finite

* Corresponding author. Present address: Department of Geophysics, Tohoku University, Sendai, Japan.

E-mail addresses: nolet@princeton.edu (G. Nolet), zhao@aob.geophys.tohoku.ac.jp (D. Zhao).

number of sources (earthquakes and occasionally nuclear test explosions) and an even more limited number of receivers. Worse, most of the receivers are located on land, leaving the oceanic areas largely uncovered. The fact that the seismic waves follow paths that are not straight, and that the wavelengths of seismic waves are of the same order as the scale length of the heterogeneities we wish to image adds another level of complexity. Notwithstanding these difficulties, the method of seismic tomography has blossomed near the end of the twentieth century: improvements in the theory of interpretation, expanding networks of high-quality stations with broadband response, and a high degree of cooperation through international data centers (IRIS in the US and ORFEUS in the Netherlands) led to ever increasing detail of global tomographic models.

Since plate boundaries dominate the global seismicity, it comes as no surprise that subduction zones are easier to image than anomalies elsewhere; in particular, their counterpart in the mantle flow – plumes – are supposedly narrow, away from seismically active areas, therefore difficult to image. A breakthrough in slab tomography was the discovery that many oceanic plates are able to penetrate the 670 km discontinuity (van der Hilst et al., 1991). This finding has been widely interpreted as evidence for ‘whole mantle convection’, though that may turn out to be somewhat of an over-interpretation, and the exact nature of the return flow remains elusive. Yet mass flux through the 670 discontinuity must be balanced either by a return flow, or by a change in the depth of the 670 discontinuity. In the latter case, the changed T–P conditions at the phase boundary will eventually return the discontinuity to the depth dictated by the phase equilibrium, thus providing a hidden return flow that has little to do with the concept of whole-mantle convection. In the case where the return flow is explicit, its character remains to be determined. Davies (1998) favors a distributed flow, with independent return flows for plumes and slabs. This view is in agreement with the very low contribution of the plume heat flux to the total heat flux of the Earth as inferred from dynamic topography (Sleep, 1990; Davies, 1990). However, Bunge (2005) argues that the geotherm is subadiabatic, leading to an underestimate for deep heat flux from surface buoyancy, and advocates a larger role for plumes in heat transport. Nolet et al. (2006) reach a similar conclusion from early tomographic images of mantle plumes. Clearly, it has become important not just to obtain images of plumes but also to get reliable information on their size, shape and temperature anomaly. In this paper we take stock of the present state of affairs of plume imagery.

2. Plume images in recent tomography

Until recently, seismic tomography provided little direct evidence for lower mantle plumes. The existence of the African and Pacific ‘superplumes’ – vast piles of material with lowered seismic velocity and probably a higher density – was uncontested (e.g. Romanowicz and Gung, 2002), but as recently as 2003 Ritsema and Allen concluded: “Whole-mantle plumes are well established through both numerical and analog experiments, but conclusive evidence for their existence remains elusive on Earth” (Ritsema and Allen 2003). At that time the first, still tentative, images of plumes were appearing in the literature (Bijwaard and Spakman, 1999; Goes et al., 1999; Zhao, 2001; Rhodes and Davies, 2001), but agreement between different models was poor. One of the major hurdles is the (presumed) narrow conduit of plumes, which makes it easy for seismic waves to diffract around them, thus masking any delay acquired by the wave energy that actually travels through the plume by earlier arrivals that have found a way around the low velocities.

More recently, a new approach to seismic inversion that compensates for the effects of wave diffraction (Dahlen et al., 2000) has led to the imaging of more than a dozen lower mantle plumes by Montelli et al. (2004), who used the delays of seismic P-waves in two frequency bands, thus exploiting the different sensitivities to diffraction as a function of seismic wavelength. The new method, officially named ‘finite-frequency’ tomography, but sometimes referred to as ‘banana-doughnut’ inversion because of the peculiar shape of the integral kernels involved, is not uncontested (de Hoop and van der Hilst, 2005a,b; Dahlen and Nolet, 2005; van der Hilst and de Hoop, 2005; Montelli et al., 2006a). However, ample testing on synthetic seismograms has demonstrated its mathematical correctness (Hung et al., 2000). Montelli et al. (2004) showed the effect of the new theory on a data set of one low frequency band only, whereas the addition of higher frequencies led to the imaging of more than a dozen well-resolved lower mantle plumes by Montelli et al. (2004), and recently Montelli et al. (2006b) have confirmed these P-wave images with a study of an independent data set comprised of long-period S-waves. At the same time, whole-mantle tomography using the traditional ray theory and a large number of different ray trajectories for (reflected and transmitted) waves in the mantle and outer core has also revealed many lower-mantle plumes under major hotspots (Zhao, 2004; Lei and Zhao, 2006).

Figs. 1 and 2 show the rapid progress in seismic tomography over the past few years. To make a direct

comparison between anomalies in P and S velocity possible (Fig. 1A, B and C, D respectively) the seismic velocity has been translated into temperature using

estimates of the velocity-temperature derivative (Nolet et al., 2006). Of the four models, PRI-P05 in Fig. 1A is the best constrained image, using P, pP and PP delay time

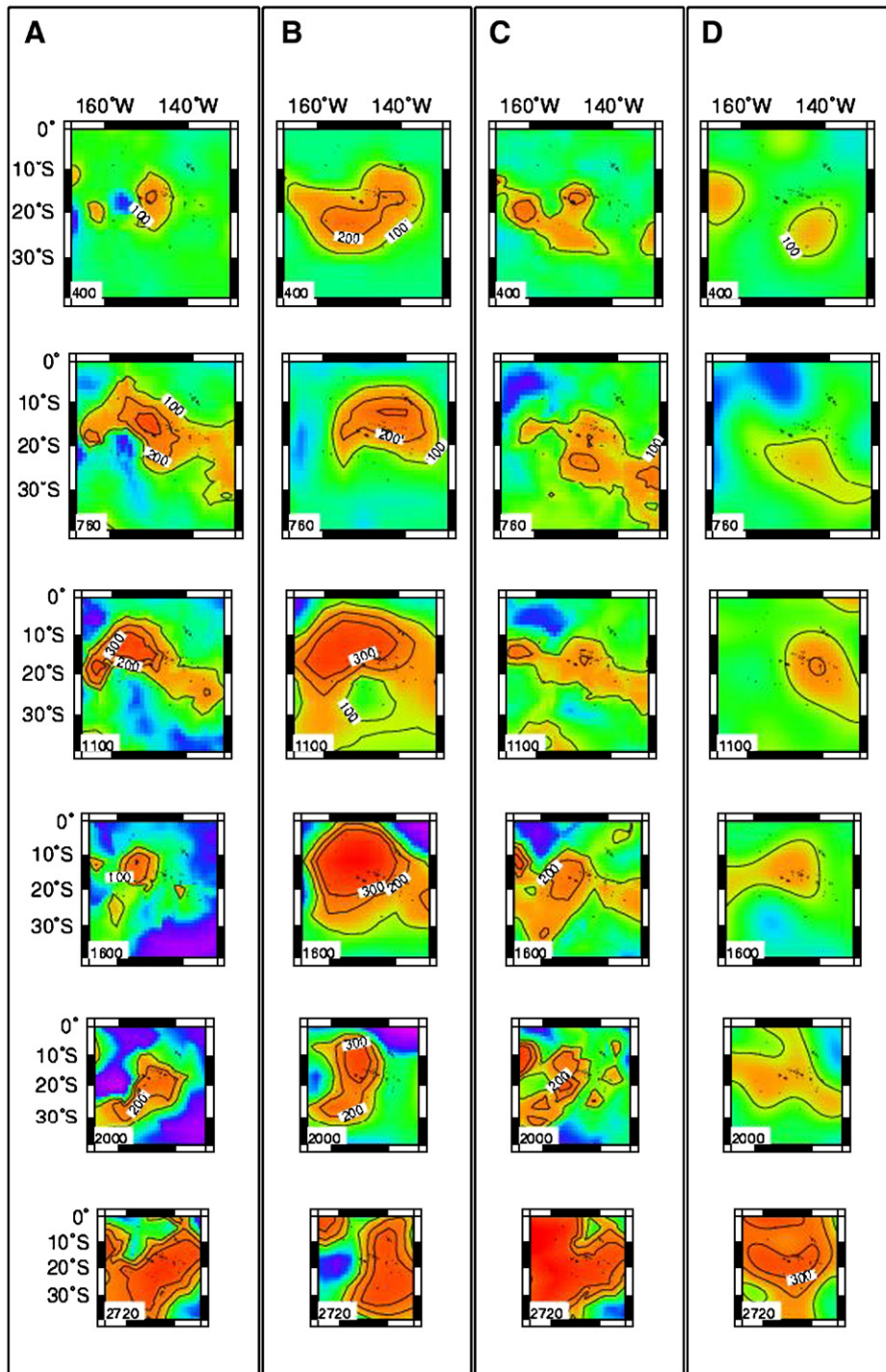


Fig. 1. Four different tomographic images of the Tahiti plume, after translating seismic velocity anomalies into temperature: (A) model PRI-P05 and (C) PRI-S05 (Montelli et al., 2006b). (B) a P-wave model by Zhao (2004) and (D) model S20RTS from Ritsema et al., 1999). Depth is indicated in km, temperature anomaly contours are in Kelvin.

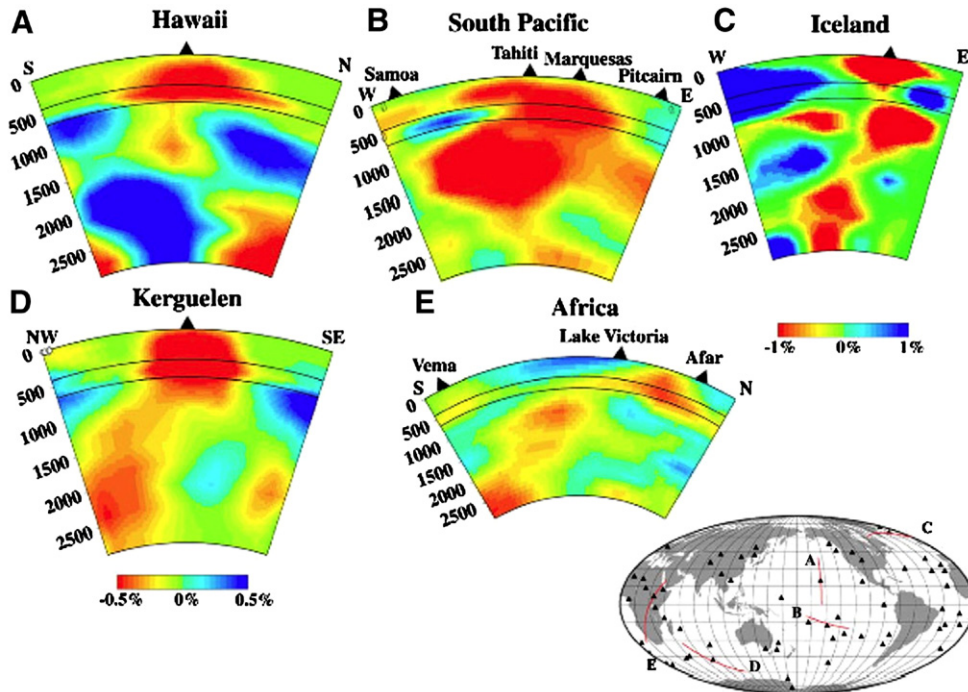


Fig. 2. P-wave tomographic images from the surface down to the core-mantle boundary under (a) Hawaii, (b) South Pacific, (c) Iceland, (d) Kerguelen, and (e) Africa derived from the global tomographic model of Zhao (2004). Locations of the cross sections are shown on the world map. The color scale ranges from -0.5% (red) to $+0.5\%$ (blue) for cross sections A, C and D, and from -1% (red) to $+1\%$ (blue) for cross sections B and E. Solid triangles denote the locations of the surface hotspots.

data in two frequency bands and finite-frequency theory. The model by Zhao (2004) in Fig. 1B was constructed with high frequency data only using ray theory, but including PcP and Pdiff waves in addition to P, pP and PP. PRI-S05 and S20RTS (Ritsema et al., 1999) are both derived from long period S-waves, but PRI-S05 uses finite-frequency theory to correct for effects of diffraction. Although the details of the low velocity anomaly beneath Tahiti are different in each of these models, a low velocity conduit consistently extends through the lower mantle. The Tahiti plume is the strongest plume visible in the lower mantle. Clearly, the use of two different frequencies in PRI-P05 leads to a much more constrained plume conduit, which is to be expected when using frequencies with different sensitivity to the size of the anomalies. The PRI models are the most recent in this sequence. S20RTS is the oldest of the four models and probably suffers from the fact that fewer broadband data were available at the time, in addition to the fact that wave diffraction affects the amplitude of the observed anomaly.

Resolution of structure in the upper mantle can be improved through the use of regional seismic networks. Temporary deployments of dense networks have

provided detailed images of low-velocity upwellings beneath Iceland and Yellowstone. In the case of Iceland a vertical low-velocity conduit is imaged from ~ 400 km depth up to 200 km where the anomaly spreads out beneath the lithosphere (Allen et al., 2002a). Beneath Yellowstone, a similar low-velocity conduit is observed. It is weaker than beneath Iceland and has a dip to the west-northwest (Waite et al., 2006). As the depth resolution of regional tomography is limited to the upper mantle, these models cannot be used to argue directly for the existence or absence of whole-mantle plumes. However, the improved resolution of upper mantle structure can be used to determine how these upwellings interact with overlying lithosphere, and can be used to test for consistency with geodynamic models of various modes of upwelling as in the case of Iceland (Section 3.4).

3. Frequently asked questions

The shape of this article was conceived by our experience at the multi-disciplinary Chapman conference ('The Great Plume Debate') in Scotland, September 2005, where the same questions regarding

tomographic images of elusive objects such as plumes kept being asked. We followed up by inviting the conference participants to submit their lists of questions by electronic mail. In this section we have grouped the most frequently asked questions into subsections.

3.1. Resolution of seismic tomography

Question: What is the spatial resolution of tomographic images in the upper mantle?

The resolution of any specific tomographic image is dependent on the dataset and tomographic technique used, and can be determined using resolution tests, which are discussed later. However, some general rules of thumb for resolution of different types of study are perhaps useful as a guide.

3.1.1. Surface waves

Many tomographic studies of the upper mantle use surface waves. The horizontal travel paths of surface waves allow resolution of primarily S-velocity structure beneath regions where there are no or few earthquakes and seismometers, e.g. beneath the oceans. Away from dense seismic networks the horizontal resolution is usually determined by the density of crossing ray paths and is therefore dependent on the specific geometry of the dataset. In this situation resolution tests – as described later – can provide information on the size and geometry of structures that can be resolved for a particular ray-path coverage. Even when a dense seismic network is available, typically on the continents, the horizontal resolution is theoretically limited by the width of the Fresnel Zone, w_F , which is approximately equal to $\sqrt{\lambda L}$ at its widest point half way between the source and receiver. L is the path length and λ is the wavelength, equal to the product of wave velocity and the period of the wave. Continent-scale models typically use periods of ~ 100 s and path lengths of ~ 3000 km (e.g. van der Lee and Nolet, 1997; Debayle and Kennett, 2000; Simons et al., 2002) which correspond to a w_F of ~ 1200 km. Regional scale experiments typically use higher frequencies and shorter paths. In the recent Iceland HOTSPOT experiment surface waves at periods of 30 to 10 s were used with path lengths of 100–300 km (Allen et al., 2002a,b), reducing w_F to 50–150 km.

While the higher frequencies improve the horizontal resolution, they also reduce the maximum depth that can be resolved. Only the crust and uppermost mantle can be resolved with 30 to 10 s period waves. Surface waves at a given frequency are sensitive to a wide depth range, but the peak sensitivity of the dominant fundamental

mode is at a depth of approximately $\lambda/3$ for Rayleigh waves and $\lambda/4$ for Love waves. They have reasonable sensitivity to a depth of about twice the peak depth. When using 100 s surface waves, the peak sensitivity for Rayleigh and Love waves is at depths of ~ 150 and ~ 110 km and they can resolve structure to depths of ~ 300 and ~ 220 km respectively. Resolution can be extended to greater depths using higher-mode surface waves, which requires more complex analysis but can be done, e.g. by fitting the seismic waveforms in the time window following the arrival of the SS wave using a summation of either surface wave modes (Nolet, 1990), or coupled normal modes (Li and Romanowicz, 1995). Using higher mode surface waves, sensitivity can be extended to the transition zone but is still limited to the upper mantle. The depth resolution for surface waves is considerably better than the lateral resolution. When surface waves with a range of different frequencies are used, the depth resolution is typically tens of kilometers, meaning that a velocity anomaly at 50 km depth can be distinguished from one at 100 km.

In summary, continent-scale surface wave studies can resolve lithospheric and asthenospheric structure to 300–400 km depth with vertical resolution at the scale of tens of kilometers and lateral resolution at the scale of ~ 1000 km. Resolution can be improved using dense regional networks and higher frequencies, but this higher resolution is only obtainable for shallower depths.

3.1.2. Body waves

While surface waves have horizontal paths, body waves through the upper mantle have predominantly vertical paths. This means that body-wave constraints are the natural complement to surface-wave datasets as they can significantly enhance the lateral resolution (Ritsema et al., 1999; Allen et al., 2002a,b). Body-wave studies also provide constraints on both P- and S-velocity structure but require stations above the study region. The Fresnel zone narrows down towards the receiver, and high frequency body waves can, in principle, resolve horizontal variations adequately with resolution comparable to that of the station spacing or even higher when both direct and reflected waves are used (e.g., Zhao et al., 2005). The vertical resolution of all tomographic studies is dependent on the extent to which the travel paths of the seismic energy (i.e. ray paths) cross each other. When using body-waves alone, the number of crossing paths is increased by three factors: having a range of epicentral distances, a range of back azimuths, and as large a number of stations over as wide an area as possible. The angle of the ray path to the

vertical is a function of the epicentral distance. Typical teleseismic studies use P- and S-wave arrivals at epicentral distances of 30° to 90° as well as phases that travel through the Earth's core (i.e. PKP, PKIKP and SKS). In the upper mantle, P- and S-wave travel at angles between $\sim 25^\circ$ and $\sim 45^\circ$ to the vertical, whereas the core phases are all within $\sim 20^\circ$ of vertical. The maximum depth that can be resolved is determined by the aperture of the network being used. If straight, ray paths at 45° to the vertical from both ends of an array will cross at a depth of $a/2$ beneath the center of the array where a is the network aperture. In the real earth, the bending of rays cause a slightly more complicated depth dependence; for example, P-wave arriving at an epicentral distance of 36° cross at a depth equal to the array span a . In practice, this is the maximum depth that can be adequately resolved. The use of finite frequency kernels (a.k.a. banana-doughnut kernels) does extend the depth resolution due to the finite width of the kernels (e.g. Hung et al., 2004), but the larger volume of the kernels at these greater depths may also reduce the spatial resolution. Fig. 3 shows two resolution tests that illustrate how the depth extent of resolution varies with the network aperture.

Question: And what can we resolve in the lower mantle?

Surface waves do not reach into the lower mantle, but the discrete normal modes of the Earth do, at the expense of a further lengthening of horizontal wavelength (1000 km or more) and the resulting loss of horizontal resolution. The seismic wavelength poses a theoretical limit to the resolution, in the sense that objects much smaller than the width of the Fresnel zone cannot be recovered even with finite-frequency tomography. Useful resolution – certainly if we wish to image narrow objects like mantle plumes or slab fragments – can thus only be obtained using body waves, possibly in addition to normal mode frequencies. It would thus pay to go to ever and ever higher frequency but teleseismic frequencies are limited by anelastic attenuation. As a rule of thumb, the shortest wavelength, λ , for both P-wave and S-wave studies of the lower mantle is about 10 km. Teleseismic rays typically have lengths between 5000 and 10,000 km, leading to $w_F \approx 200$ –300 km for the highest frequencies. The major limitation to body-wave resolution in the lower mantle is therefore the path coverage, which is still poor in many regions of the lower mantle.

Question: What are the realistic limitations of the technique? Or, put another way, what can we expect in the future?

Finite-frequency tomography has no difficulty correcting for the diffraction effects of objects about half

the Fresnel width (Hung et al., 2000), and so it seems the shortest wavelengths available could in principle be used to give details even of plume conduits. However, using short wavelengths in order to resolve narrow anomalies is not only a blessing, but also a curse: if the raypath 'misses' the plume it will not sense the anomaly. Especially in the Southern hemisphere, path coverage is sparse and the larger width of a low-frequency wavepath pays off by providing sensitivity in regions not covered by the raypath as computed by Snell's law. Efforts are currently under way to re-measure travel time delays in a range of frequency bands, thus fully exploiting finite-frequency effects (Sigloch and Nolet, 2006). Waveform inversions of the kind proposed theoretically by Tromp et al. (2005) are a generalization of the finite-frequency ideas, and should lead to even better exploitation of the information in a seismogram. Such methods however are nonlinear, require massive compute power, and have yet to show their practical feasibility.

In summary, therefore, the theoretically obtainable resolution is high (even better than 100 km) where the Fresnel zone is narrow, i.e. in the upper mantle, or at depth if raypath coverage is dense and finite-frequency theory is used in the interpretation. If the geophysical community is able to launch a major effort to cover the oceans with seismic sensors, a resolution of about 200 km should be feasible for the entire lower mantle. This, however, would involve investments comparable to those spent for the first human explorations at the surface of the Moon. More realistically, a limited increase in coverage, coupled with advanced interpretation methods for waveforms or delays in different frequency bands, may eventually lead to a resolution of the order of 400 km in selected regions of the lower mantle. A theoretical limit is imposed by the minimum wavelength of seismic waves which leads to irrecoverable loss of signal for anomalies much smaller than the Fresnel zone; in practice this means that anomalies much smaller than about 200 km in the lowermost mantle – of the order of 100 km if finite-frequency theory is used – can never be resolved with seismic tomography.

Question: How does one estimate the actual resolution in a tomographic image?

Not all the fast and slow anomalies visible in a tomographic image are reliable features, and the amplitude of an anomaly is usually less well constrained than its shape. Even a well-resolved tomographic image can be affected by the type of model parameterization (grid nodes, blocks, spherical harmonics), and the limitations imposed by it, as well as by damping and

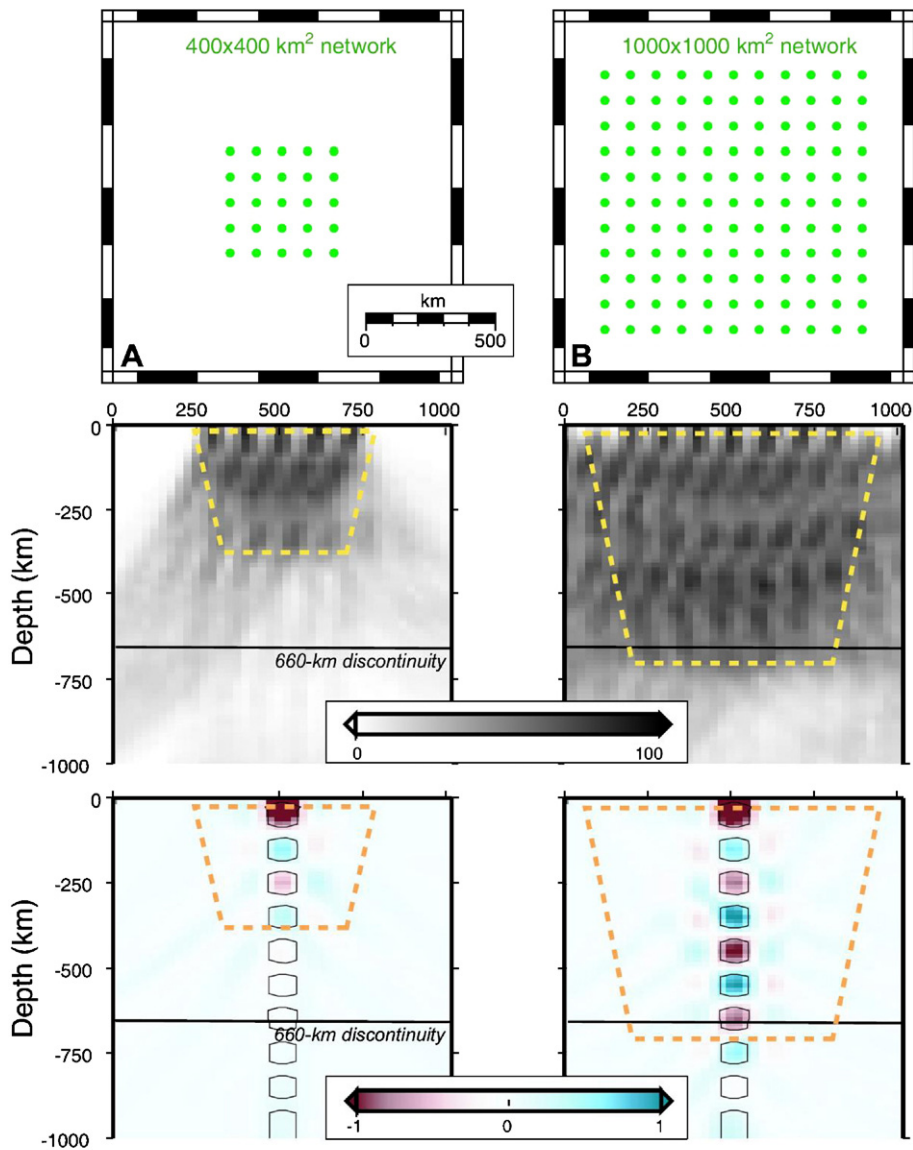


Fig. 3. Illustrations of velocity resolution that can be obtained by teleseismic travel time tomography using (A) a $400 \times 400 \text{ km}^2$ network and (B) a $1000 \times 1000 \text{ km}^2$ network. The top panels show the network configuration, the middle panels show P and PKIKP ray density in the upper 1000 km of the mantle beneath the networks, and the bottom panels show the recovery of 100 km thick alternating high and low velocity anomalies after inverting synthetic data based on the ray density shown above. The ray density is that obtained by a 2 year deployment in Iceland. The dashed lines indicate mantle regions where ray density and hence model resolution is highest. Although the earthquake distribution around Iceland was used for this test, the results are representative of the resolution possible with wide-aperture regional networks.

smoothing operations used to stabilize the inversion. When a data set has a dense and uniform ray distribution (such as in local or regional tomography in Japan and California), a smaller grid can be used to image a detailed structure and light damping and smoothing can be adopted to better recover the amplitude of velocity anomalies (e.g., Zhao et al., 1992). In the case of global tomography, the ray density and crisscrossing is very

heterogeneous, and so a coarse grid has to be used and strong damping and smoothing are required to stabilize the inversion process. Many global tomographic images are ‘low passed’ versions of the true Earth and deliberately exclude wavelengths below a certain limit (typically $\sim 1000 \text{ km}$) to gain stability in the images.

Since the ray density and the degree of ray crisscrossing vary everywhere in the model, the spatial

resolution and reliability of the tomographic image change from place to place. To evaluate whether a feature is reliable or not, it is necessary to perform a specific resolution analysis for that feature. Tomographers use “sensitivity tests” to evaluate the reliability of a feature of interest. This is done as follows: first, a synthetic input model is constructed that includes the feature to be examined (either a slab or a plume) with its geometry similar to that appearing in a real tomographic image. Secondly, synthetic data (e.g. travel times) are calculated for the synthetic input model. The numbers of stations, earthquakes and rays are the same as those in the real data set, and the same computational algorithms are used. To simulate the observation errors in the real data, (random) noise is also added to the calculated synthetic data. Thirdly, the synthetic data are inverted using the same inversion algorithm as that for the real data. Finally, the inversion result is compared with the input synthetic model to see whether and how well the assumed feature is recovered. If the general geometry of the feature is reconstructed, then it is considered to be “reliable”, though the amplitude of the velocity anomaly is generally not fully recovered because of the damping and smoothing. If this is repeated using different realizations of the random noise, we also obtain an impression of the influence of data errors. Examples of such synthetic tests can be found in Zhao (2001, 2004) and Montelli et al. (2004, 2006b).

Tomographers also use so-called “checkerboard resolution tests” (CRT) to evaluate the resolution of a tomographic image. The CRT is a generalized form of the resolution test. The input model resembles a checkerboard with alternating positive and negative anomalies. One conducts the checkerboard tests with different grid spacings (or block sizes). The CRT is useful to view the reliability of the entire modeling space, but it is not sufficient to judge whether a special feature (like plume or slab) is resolved or not. Generally, tomographers conduct both types of synthetic tests to examine the overall resolution scale of the entire model as well as the reliability of some specific features such as a slab or a plume.

Question: How does one judge if an observed tomographic anomaly is resolved?

This is often the most difficult question for the non-seismologist to answer if one is using results from a published tomographic paper. Here are some aspects to watch out for:

What type of data is being used in the inversion? If surface waves are used, the maximum depth of resolution is about $2\lambda/3$ for Rayleigh waves, $2\lambda/4$ for

Love waves, deeper if higher modes are used. If body-waves are being used, to what extent are the ray-paths crossing in the region of the anomaly? Both azimuthal variation and epicentral distance variations result in crossing paths along with the use of different phases, i.e. mantle and core phases. Beware of anomalies at the edge of the resolved region as they may be structures smeared into the model.

Is smearing a problem? Does the velocity anomaly have a structure similar in geometry to the sensitivity of the dataset being used? Examples include elongated anomalies along body-wave ray paths or horizontal stripes along surface wave paths.

Are there resolution tests? Do they support the assertion that the observed anomaly is real? Resolution tests, using synthetic velocity anomalies that are both similar and different in geometry to the observed anomaly, are important. Spike, blob or checkerboard tests indicate the scale of anomaly that can be resolved and also illustrate the extent of smearing. Tests using an anomaly of similar geometry to the observed anomaly can indicate the effects of smoothing and damping. Beware of resolution tests that only use a synthetic model with the same geometry as the observed. If an observed anomaly is the result of smearing true Earth structure along ray paths, the reconstructed anomaly will have extra smearing in the resolution test but this is not always clearly recognizable.

Question: Does the absence of an anomaly in a tomographic model imply that there is no such velocity structure in the Earth?

Again, we feel this is best answered by providing a checklist:

What is the model resolution? To argue that a structure is absent requires demonstration that it would be resolved if it existed. A resolution test demonstrating the resolvability of the allegedly absent anomaly is necessary.

Is the seismic wavefield observed at the surface sensitive to the allegedly absent structure? The rules of thumb regarding the wavelengths and Fresnel zones that we discussed earlier may give a useful first order answer. More exact answers require a test that goes beyond the computational algorithm being used (e.g. shortcomings of ray theory will not be visible in a resolution test using ray theory). A test using full waveform propagation, such as the spectral element method (SEM) is the best way to answer this question.

Unfortunately, there is no simple test to answer the question. Accordingly, it is much more difficult to argue that an absent anomaly means there is no velocity structure in the mantle, than to demonstrate that an

imaged anomaly is real Earth structure. This issue has played a major role in the debate over the existence or absence of plumes in the mantle: does the absence of a plume conduit in a tomography model demonstrate that a plume is not present?

3.2. Imaging artifacts

Question: To what extent does the interpretation depend on the initial model assumptions? i.e., if you are looking for plumes, are you more likely to find them?

Since the inverse problem is invariably underdetermined, there is an infinite number of models that satisfy the data at the same level of χ^2 , or misfit. Thus, tomographers cannot escape making a subjective choice among them. The usual choice is to stay ‘closest’ to the initial model, a strategy that lends itself to algorithmic simplicity but that is still not unique because there are different mathematical definitions of ‘closest’. Most tomographic models represent either the smallest or the smoothest perturbation to the initial model that makes the model fit the data to a prescribed level of misfit. Thus, there are certain aspects of tomographic images that depend strongly on the initial model, but plumes are not among those. The explanation is simple. The initial model is almost always a spherically symmetric model, and whereas the horizontal layering (e.g. the presence of a Lehmann discontinuity) may influence the tomographic result by compensating for the presence or absence of a layer, vertical continuity of positive or negative anomalies could only be induced with a highly anisotropic vertical smoothing, but we know of no tomographic model constructed that way. The parameterization of the model may influence the sharpness of structures (e.g. if one densifies the grid in seismically active regions such as subduction zones), but again this would not induce plume-like artifacts. The models by the Princeton group (Montelli et al. 2004, 2006b) are all constructed with a randomized grid of nodes and isotropic smoothing towards model IASP91. The model of Zhao (2004) is constructed with a regular grid with optimal damping and smoothing towards model IASP91 and with the depth variations of the Moho, 410 and 660 km discontinuities taken into account in the tomographic inversion, but these would not cause plume-like artifacts in the mantle (Zhao, 2001, 2004).

Question: To what extent is the discovery of a plume beneath an ocean island an artifact of receiver siting, or a real observation?

The presence of an ocean island station above an imaged plume results in a bundle of body-wave ray-

paths below the station that could potentially cause vertical smearing of a low-velocity anomaly in the region. This leads to the above question. Although there is the potential for a smearing artifact to look like a plume in the upper mantle, it is not a concern in the lower mantle as any vertical conduit in the lower mantle is mainly resolved by almost horizontal ray paths to distant stations.

If a plume image in the upper mantle starts as a narrow plume right beneath the station, and spreads out with depth to reach a width of hundreds of km in the transition zone, it is a sign that a low velocity region is present but also that its shape is not resolved: in the absence of any further constraints the image simply follows the raypath geometry. This danger is significantly reduced when finite-frequency theory is used in the interpretation, since the actual sensitivity is spread out over a region as wide as the Fresnel zone, and is zero at the location of the geometrical raypath. Zhao (2004) used various reflected and diffracted waves (pP, PP, PcP, and Pdiff) in the mantle in addition to the first P-wave so that ray path coverage is improved significantly and tests show that the final tomographic image is not sensitive to the presence of an ocean island station. Lei and Zhao (2006) further used some waves passing through the outer core to improve the tomographic resolution in the mantle.

Montelli et al. (2006a) study a related issue: the role of crustal corrections. Since crustal structure cannot adequately be resolved with teleseismic P-wave, one usually applies such corrections using all available knowledge about crustal thickness. If ray theory is used for an island station correction, the predicted arrival is fast because it travels through basaltic rock until it reaches the station. The true wave is somewhat influenced, i.e. slowed down, by the presence of water away from the geometrical raypath. This can indeed cause a negative velocity artifact in the shallow mantle. Finite difference computations for very small islands (20 km wide) show that the neglect of finite-frequency effects in the station correction for a long period P-wave may induce a negative upper mantle anomaly of the order of 0.3%. This is still well below observed upper mantle plume anomalies, which are of the order of 1–2%. For larger islands such as Kerguelen or Reunion the effect is negligible.

3.3. Interpretation of tomographic anomalies

Question: To what extent can the tomographic anomalies be attributed to composition rather than simply to temperature?

The seismic velocity anomalies imaged in tomography experiments could be the product of temperature anomalies, compositional variations (including volatiles), the presence of partial melt, or anisotropy. Seismic wave propagation is primarily sensitive to two resolvable parameters, the P- and S-wave velocity. There is also a weaker sensitivity to attenuation, which has been more difficult to extract, although advances are now being made. Given the small number of resolvable seismic parameters and the large number of potential sources of their variation, we must ask two questions when interpreting seismic velocity structure: What is the most likely cause of velocity anomalies, and what is the possible range of interpretations?

Using the range of petrologic models proposed for the bulk composition of the upper mantle, as well as reasonable estimates for possible temperature variations and likely melt volumes, estimates of the resulting velocity anomalies can be made. Goes et al. (2000) calculate the amplitude of velocity anomalies expected in the upper 200 km of the mantle given the likely range of compositions and temperatures beneath Europe. They conclude that when the mantle is below the solidus, temperature is the key source of velocity anomalies because a 100 °C temperature anomaly would result in a decrease of 0.5–2% in the P-velocity and 0.7–4.5% in the S-velocity while compositional variations all result in <1% variations. Above the solidus, the effect of partial melt is significant and difficult to quantify as it is very sensitive to the geometry of the melt, i.e. whether it is in thin films along grain boundaries or more spherical pockets.

Given the greater sensitivity to temperature, most velocity anomalies are initially interpreted in terms of temperature anomalies. Interpretation in terms of compositional variations, partial melt or fluids requires justification. In cases where constraints on both the P- and S-velocity of an anomaly are available, the hypothesis that temperature alone is the source of the anomaly can be tested. If rejected, the case for compositional effects, partial melt or fluids can be made. This approach has led to identification of shallow regions that likely contain partial melt beneath the continents (Goes et al., 2000; Goes and van der Lee, 2002) and also to the hypothesis that partial melt or fluids reside deep in the mantle beneath Iceland (Allen and Tromp, 2005). Recent work by Faul and Jackson (2005) on the temperature dependence of S-velocity for realistic seismic frequencies has however shown that even a decrease as large as 8% does not require the rock to be partially molten.

The uncertainty in the true amplitude of a seismic anomaly imaged using tomography is a significant

source of error in any interpretation of temperature of compositional variations. As described in the resolution section, smoothing and damping in the inversion, and wavefront healing (which is accounted for in finite-frequency inversions but not in ray-theoretical inversions), all reduce the amplitude of observed velocity anomalies. An alternative approach is to test if physical models based on other, non-seismic, datasets are consistent with the seismic data.

In the lower mantle there is a narrower range of major minerals, but a larger uncertainty regarding the seismic velocity as a function of variation in the ambient temperature. The likely major constituent is MgSiO₃ perovskite, along with (Mg,Fe)O magnesiowüstite. The anharmonic (i.e. valid at very high frequency) temperature derivative $\partial V_p/\partial T$ of this composition is only approximately known (Karki et al., 2001; Wentz-covitch et al., 2004; Aizawa et al., 2004). At seismic frequencies, the anelastic contribution to $\partial V_p/\partial T$ cannot be neglected and adds to the uncertainty. Thus, only rough estimates can be given: a rise of 100 K will lower V_p at the top of the lower mantle by about 0.3–0.4%, and by about half that value in the lowermost mantle.

Probably the most important compositional uncertainty is the possibility of a significant iron enrichment of the lower mantle (Forte and Mitrovia, 2001; van der Hilst and Kárason, 1999; Morse, 2000; Kellogg et al., 1999; Nakagawa and Tackley, 2004). If the iron abundance $X_{Fe} = (Fe)/((Mg)+(Fe))$ is increased by 0.01, this will lower V_p by about 0.2% (Stixrude et al., 1992; Kiefer et al., 2002). Thus, on the face of it, a midmantle plume anomaly of, say, –0.5% could be interpreted assuming either a 200 K rise in temperature or an excess iron abundance of 0.025. However, the latter option raises geodynamical problems for the interpretation of plume-like anomalies, because the added density of about 0.3% for every increase of 0.01 in the abundance of iron (Weidner and Wang, 1998) is considerable and would almost certainly inhibit the rising of a plume if a significant part of the anomaly is due to iron enrichment.

The possible role of water is unknown. It probably affects the seismic velocity mostly through anelastic effects (Karato, pers. comm. 2005). Water may enhance grain growth, thereby minimize grain size-sensitive viscoelastic relaxation (Solomatov, 2001; Korenaga, 2003), thus unexpectedly raise rather than lower V_p, but no pertinent experimental or theoretical results are available at this time.

In summary, a temperature interpretation seems the most straightforward explanation for lower mantle plume anomalies, with a possible role for volatiles left open.

Question: How can one judge if the interpretation of the velocity anomaly in terms of temperature, composition or melt is reasonable?

To answer this, one should look for the following aspects:

Is the interpretation unique? The answer is usually no, therefore the question becomes: What other constraints are applied? What is the justification for a “preferred” interpretation? It may be the simplest, perhaps assuming a temperature generated anomaly, or it may be based on other models for the region, e.g. geochemical or geodynamic.

Has the likely range of true velocity anomalies been taken into account? While the model slice presented may show a peak S-velocity anomaly of 2%, what is the likely range of the true velocity anomaly considering the resolution of the tomographic inversion?

Question: How should one interpret images of plumes that appear to originate in mid-mantle?

Whereas the observation of a negative anomaly with vertical continuity is a strong indication for the presence of a plume, the absence of an anomaly is more difficult to interpret. Resolution calculations by [Montelli et al. \(2004\)](#) indicate that no plume with a radius less than 100 km would be detectable with the data on hand, and very few are resolvable if the radius was as small as 200 km. The absence in the image can thus be interpreted as a true absence or as a narrowing down of the plume. Also, the temperature derivatives of V_P and V_S decrease in magnitude with depth, such that the same temperature anomaly gives a weaker velocity anomaly, that may become invisible. On the other hand, if viscosity increases with depth – as is likely at least in mid-mantle – one would expect an active plume to widen, rather than narrow down with depth. [Montelli et al. \(2006b\)](#) therefore conclude that such plumes probably all represent a ‘dying’ stage, i.e. they have depleted their source region.

3.4. Case study I: Iceland

As one of the classic plume locations, Iceland has been the focus of many studies designed to constrain the source of the voluminous volcanism responsible for the island, and there has been a great deal of debate about the interpretation of these studies. Here we will use Iceland as an example of a difficult interpretation. The tomographic constraints on the processes responsible for Iceland fall into two categories: (1) those that use global datasets to constrain structure beneath Iceland, and (2) those that use regional seismic data recorded at stations on Iceland. The regional seismic studies provide

constraints on the upper mantle only, while global studies are needed to constrain the lower mantle.

Global images of the lower mantle beneath Iceland have been used to draw contradictory conclusions about the origin of Iceland. However, it is not clear that the tomographic images themselves are inconsistent. While all models show a large low velocity anomaly in the upper mantle (e.g. [Ritsema et al., 1999](#); [Megnin and Romanowicz, 2000](#); [Karason and van der Hilst, 2001](#); [Montelli et al., 2004](#)), only a small subset point to a continuation of the anomaly in the lower mantle ([Bijwaard and Spakman, 1999](#); [Zhao, 2001, 2004](#)). Whether these models are contradictory or not is dependent on the resolution of each model in the lower mantle and the robustness of any anomaly that is observed. The ring of earthquake sources and seismic stations around the Pacific Ocean makes the lower mantle beneath the Pacific one of the best-resolved regions of the lower mantle. In contrast, fewer rays sample beneath the Atlantic, making lower mantle resolution more difficult in the case of Iceland, though the use of reflected waves from the core-mantle boundary (PcP) can improve the resolution in the lower mantle (e.g., [Zhao, 2001, 2004](#)).

This resolution problem is illustrated in [Foulger et al.’s \(2001\) Fig. 19b](#), which shows a resolution test of the [Karason and van der Hilst \(2001\)](#) global tomography model. The [Karason and van der Hilst \(2001\)](#) model shows a low velocity only in the upper mantle beneath Iceland, but the resolution test illustrates that if the anomaly does extend into the lower mantle it could not be resolved in their model. More recently, [Montelli et al. \(2004\)](#) argued that their dataset could image a >200 km radius P-velocity anomaly in the lower mantle. The fact that it does not show such anomaly therefore suggests that the Iceland “plume” is confined to the upper mantle. The models of [Bijwaard and Spakman \(1999\)](#) and [Zhao \(2001\)](#) do point to a continuation of the low velocity anomaly into the lower mantle, and the S-velocity model of [Montelli et al. \(2006a,b\)](#) shows an anomaly in the lowermost lower mantle. In these models, however, the amplitude of the lower mantle anomaly is much smaller than in the upper mantle and the geometries of the anomalies are not simple vertical columns. While the low amplitudes may be due to modeling effects, and the dynamics of the lower mantle may result in complex upwelling geometries, the absence of a simple vertical conduit, as visualized in geodynamic models, leaves questions as to the nature of the imaged upwelling. The models of [Bijwaard and Spakman \(1999\)](#), [Zhao \(2001\)](#) and [Montelli et al. 2004, 2006a,b](#) all agree that there is no simple vertical conduit extending from the upper

mantle down through the lower mantle beneath Iceland. Therefore, the nature of any lower mantle upwelling beneath Iceland, should it exist, remains elusive.

In contrast, the upper mantle clearly contains a large low-velocity anomaly centered beneath Iceland. Regional experiments using the permanent SIL network on Iceland (Stefansson et al., 1993) and the temporary ICEMELT (Bjarnason et al., 1996) and HOTSPOT (Allen et al., 1999) networks provide increased resolution of this feature. All the regional models show a low velocity anomaly extending from the surface down to ~ 400 km depth with a diameter of between 100 km and 400 km and have been interpreted in terms of a near-cylindrical vertical upwelling (Wolfe et al., 1997; Foulger et al., 2001; Allen et al., 2002a,b; Hung et al., 2004; Allen and Tromp, 2005). In detail these images show a range of anomaly diameters and various degrees of smoothness. This is due to differences in the regularization of the tomographic inversions, i.e. smoothing distances and degrees of damping. The different body-wave datasets also play a role. One significant difference in the datasets is the inclusion of surface-waves in addition to body-waves by Allen et al. (2002a,b). The surface waves allow resolution of horizontal velocity anomalies invisible to relative arrival-time body-wave datasets when the velocity anomaly extends beneath the entire seismic network. Through the inclusion of surface-waves Allen et al. (2002a,b) image a top to the upwelling as shown in Fig. 4. They interpret their velocity model as showing

upwelling material spreading out beneath the oceanic lithosphere. Fig. 4 also shows a comparison of the velocity structure beneath Iceland with the temperature profile in the numerical convection model of Farnetani et al. (2002). In the convection model, heating at the base of the mantle results in a vertical plume which then spreads out beneath the higher viscosity lithosphere. The imaged velocity structure beneath Iceland is in close agreement with the numerical prediction of plume structure beneath Iceland.

There is no single answer to the question of how deep these regional tomography models can resolve. Below a depth equal to about half the network aperture, the resolution decreases with depth. At depths greater than the network aperture the resolution is poor. The diameter of Iceland (on which the regional seismic networks were deployed) is ~ 300 km north-south and ~ 500 km east-west. The fact that the observed velocity structure in all the models is similar above ~ 400 km is a good indication that structure is well resolved to 400 km depth. This is also illustrated in resolution tests (Wolfe et al., 2002; Allen and Tromp, 2005). Foulger et al. (2000) use their regional tomography image to argue that the low velocity anomaly beneath Iceland originates in the mantle transition zone. This argument cannot be based on an absence of the low velocity anomaly below the transition zone as the model has no resolution at these depths. Instead, it is based on the tabular structure of the low velocity anomaly they image at depths greater than 350 km. Resolution is poor at these depths and

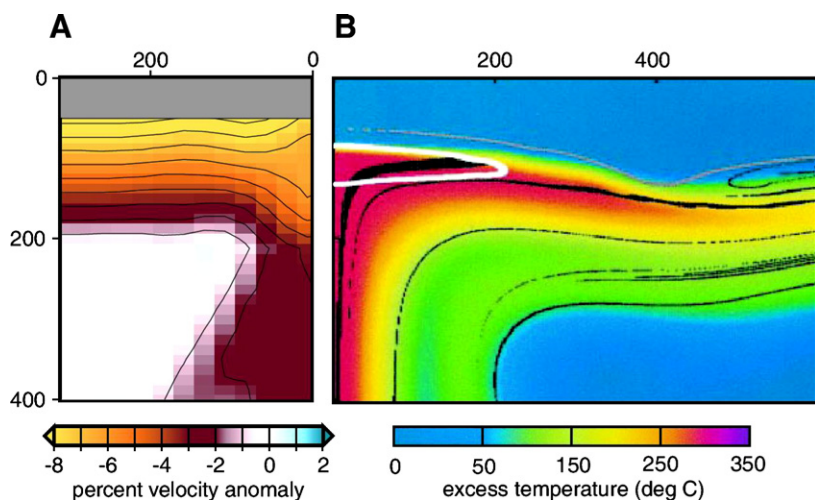


Fig. 4. Comparison of tomographically imaged velocity structure beneath Iceland with the excess temperature profile across a numerical convection model for a whole mantle plume. (A) Cross-section (oriented southwest to northeast) through the ICEMAN-S model of S-velocity heterogeneity in the upper mantle beneath Iceland of Allen et al. (2002a,b). (B) Cross-section (same scale) through the numerical plume model of Farnetani et al. (2002). The model was allowed to evolve for 40 Ma after the onset of melting. The white contour shows the region of melt formation.

other regional models using larger datasets have failed to image a similar structure so the observation remains unconfirmed.

The maximum depth resolution of the regional Iceland datasets has recently been extended to the base of the transition zone through improvement in the tomographic technique to account for finite-frequency effects. Application of the broad banana-doughnut kernels more accurately represents the width of the region to which a travelt ime measurement is sensitive. This improved representation of the sensitivity of seismic arrivals allows information about deeper structure to be extracted in the tomographic inversion. Using this approach [Hung et al. \(2004\)](#) show that the low velocity extends to the base of the transition zone. Even with these improved techniques, however, it is still not possible to use the regional datasets to determine if the conduit extends through into the lower mantle.

Massive computers and advances in numerical techniques now make it possible to propagate seismic wavefields through three dimensional velocity structures to forward calculate synthetic waveforms which can be compared to observed data. These forward calculations, such as the Spectral Element Method (SEM) ([Komatitsch and Tromp, 2002a,b](#)), do not make the simplifying assumptions used in tomographic techniques and therefore provide an opportunity to test tomographic models to see if they reproduce the observations from which they were generated. The ICEMAN models for the Icelandic upper mantle ([Allen et al., 2002a,b](#)), generated using ray theory, were tested using the SEM ([Allen and Tromp, 2005](#)). The tests show that the ICEMAN models represent an end-member in a range of velocity structures that satisfy the seismic observations. As expected, the tomographic technique broadened the vertical conduit and reduced the amplitude of the seismic anomaly. By testing different diameter upwellings the allowable range was determined to be from ~ 150 km up to 200 km in diameter. The upper limit is equal to that observed in the ray theoretical models, but the true amplitude of the seismic velocity is likely twice the ray-theoretical value. The minimum diameter of the conduit is constrained by the fact that a narrower conduit would not be observable at the surface. Wavefront healing effects would erode delays in the seismic wavefront as it approached the surface, making the travelt ime delays significantly less than those observed. Note that finite frequency inversions are less sensitive to image broadening, at least if they use a range of frequencies to exploit the sensitivity of wavefront healing to the size of the anomaly with respect to the seismic wavelength.

To summarize, while tomographic images of the mantle beneath Iceland have led to extensive debate, the various images are mostly consistent. There is a low velocity anomaly that extends through the upper mantle, which is widely interpreted as a buoyant upwelling that spreads out beneath the oceanic lithosphere. The structure of this imaged upper mantle plume is consistent with geodynamic models for whole mantle plumes. Whether this anomaly extends into the lower mantle is a continuing focus of research. In order to finally answer this question we need improved data coverage which is only obtainable using ocean bottom seismographs around Iceland.

3.5. Case study II: Hawaii

The resolution beneath Iceland is good compared to that beneath Hawaii — the disagreement in the case of Iceland is mainly whether the plume becomes too thin to detect adequately or whether it is absent completely. In this section we study a different case: a possibly strong plume in a part of the mantle that is not well covered by seismic rays. The mantle structure under Hawaii is among the most difficult to image tomographically because of the lack of seismic stations in the broad Pacific Ocean except for a few stations on the narrow Hawaiian island chain. To overcome this problem and to obtain sufficient ray path coverage in and around Hawaii, high-frequency arrival times of various reflected and transmitted waves in the mantle and outer core are used in the tomographic inversion ([Zhao, 2001, 2004; Lei and Zhao, 2006](#)). A continuous low-velocity anomaly is imaged clearly from the surface to the CMB under the Hawaiian hotspot ([Fig. 5](#)). The root of the anomaly at the CMB is located north of the Hawaiian hotspot on the surface, and the anomaly in the mantle is tilting toward the south, which is likely due to the mantle flow. Thus the location of the Hawaiian hotspot may not be stationary in the long geological history, as evidenced by the paleomagnetic and numerical modeling studies (e.g., [Tarduno and Cottrell, 1997; Steinberger, 2000](#)). It is also found that the Hawaiian plume is not part of the Pacific superplume, but an independent whole-mantle plume ([Zhao, 2004; Lei and Zhao, 2006](#)). There may be, however, heat or material exchange between them at a mid-mantle depth ([Fig. 5](#)).

Finite-frequency inversion of P- and S-waves by [Montelli et al. \(2006a,b\)](#) complicates this simple picture for the Hawaii plume though. The images of P-wave anomalies, which have a better resolution, show the Hawaiian plume split into two branches, NW and SE of the hotspot location, in the lower mantle. Such a split is

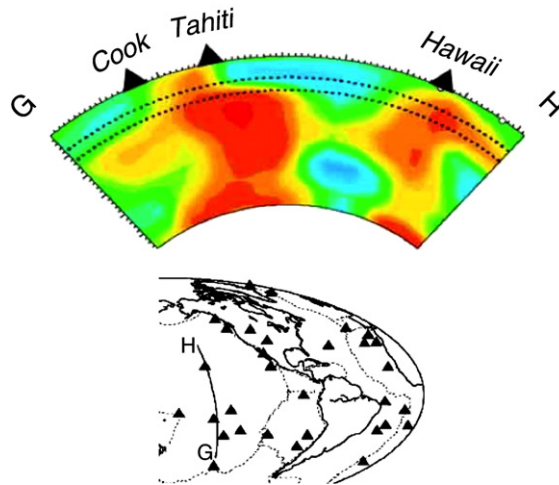


Fig. 5. A north-south vertical cross section of P-wave tomography passing through Hawaii and South Pacific (Lei and Zhao, 2006). Location of the cross section is shown on the insert map. The color scale ranges from -1% (red) to $+1\%$ (blue). Solid triangles denote the locations of the surface hotspots.

confirmed in the S-wave anomalies near 1000 km depth, but the S wave image disappears below 2000 km depth.

4. Conclusions

Every geophysical inverse problem is underdetermined, and requires a certain amount of subjective judgement from the interpreter to choose the preferred image among many options. Progress is measured by the ever increasing detail that shows up consistently among those options. Very recently, plumes have entered that realm. Though the images are still blurred and details are not the same among different efforts, there is no doubt that plumes exist in the lower mantle.

This article was written at a time that the technique of tomographic imaging is undergoing important changes. The GSN, a global network of digital, broadband seismic stations, has only recently been completed to full strength and the number of similar stations in other networks is still increasing. The broadband character of these data allows tomographers to mine the frequency dependence of seismic delays, which is a direct function of the size of anomalies with respect to the width of the Fresnel zone. The first plume images constructed with the theory of finite-frequency tomography used only a haphazard combination of two frequency bands, and is likely to be improved upon in the years to come. Increasing data coverage is also to be expected from temporary deployments both on land and in the oceans. For example, the USArray project is expected to bring in a wealth of data on the deep structure of the mantle

beneath Yellowstone. By all signs, seismic tomography is entering a Golden Age.

Acknowledgements

We thank Geoffrey Davies, Ian Jackson and Ian Carmichael for their constructive reviews of this paper. GN acknowledges support for tomographic research from the NSF (EAR 0309298). NSF also provided support for RA's contribution (EAR 0539987). DZ is supported by grants (B-11440134, A-17204037) from the Japanese Ministry of Education and Science.

References

- Aizawa, Y., Yoneda, A., Katsura, T., Ito, E., Saito, T., Suzuki, I., 2004. Temperature derivatives of elastic moduli of MgSiO_3 perovskite. *Geophys. Res. Lett.* 31, L01602.
- Aki, K., Lee, H., 1976. Determination of three-dimensional anomalies under a seismic array using first p arrival times from local earthquakes: 1. a homogeneous initial model. *J. Geophys. Res.* 81, 4381–4399.
- Allen, R.M., Tromp, J., 2005. Resolution of regional seismic models: squeezing the Iceland anomaly. *Geophys. J. Int.* 161, 373–386.
- Allen, R.M., Nolet, G., Morgan, W.J., Vogtjard, K., Bergsson, B.H., Erlendsson, P., Foulger, G.R., Jakobsdottir, S., Julian, B.R., Pritchard, M., Ragnarsson, S., Stefansson, R., 1999. The thin hot plume beneath Iceland. *Geophys. J. Int.* 137, 51–63.
- Allen, R.M., Nolet, G., Morgan, W.J., Vogtjard, K., Bergsson, B.H., Erlendsson, P., Foulger, G.R., Jakobsdottir, S., Julian, B.R., Pritchard, M., Ragnarsson, S., Stefansson, R., 2002a. Imaging the mantle beneath Iceland using integrated seismological techniques. *J. Geophys. Res.* 107, 2325. doi:10.1019/2001JB000595.

- Allen, R.M., Nolet, G., Morgan, W.J., Vogfjord, K., Nettles, M., Ekstrom, G., Bergsson, B.H., Erlendsson, P., Foulger, G.R., Jakobsdottir, S., Julian, B.R., Pritchard, M., Ragnarsson, S., Stefansson, R., 2002b. Plume driven plumbing and crustal formation in Iceland. *J. Geophys. Res.* 107, 2163. doi:10.1029/2001JB000584.
- Bijwaard, H., Spakman, W., 1999. Tomographic evidence for a narrow whole mantle plume below Iceland. *Earth Planet. Sci. Lett.* 166, 121–126.
- Bjarnason, I.-T., Wolfe, C.-J., Solomon, S.-C., Gudmundson, G., 1996. Initial results from the ICEMELT experiment: Body-wave delay times and shear-wave splitting across Iceland. *Geophys. Res. Lett.* 23, 459–462.
- Bunge, H., 2005. Low plume excess temperature and high core heat flux inferred from non-adiabatic geotherms in internally heated mantle circulation models. *Phys. Earth Planet. Inter.* 153, 3–10.
- Dahlen, F.A., Nolet, G., 2005. Comment on the paper on sensitivity kernels for wave equation transmission tomography by de Hoop and van der Hilst. *Geophys. J. Int.* 163, 949–951.
- Dahlen, F.A., Hung, S.-H., Nolet, G., 2000. Frechet kernels for finite-frequency traveltimes — I. Theory. *Geophys. J. Int.* 141, 157–174.
- Davies, G., 1990. Ocean bathymetry and mantle convection, 1, large-scale flow and hotspots. *J. Geophys. Res.* 93, 10467–10480.
- Davies, G., 1998. Topography: a robust constraint on mantle fluxes. *Chem. Geol.* 145, 479–489.
- de Hoop, M., van der Hilst, R., 2005a. On sensitivity kernels for wave equation transmission tomography. *Geophys. J. Int.* 160, 621–633.
- de Hoop, M., van der Hilst, R., 2005b. Reply to a comment by F.A. Dahlen and G. Nolet on: On sensitivity kernels for wave equation tomography. *Geophys. J. Int.* 163, 952–955.
- Debayle, E., Kennett, B.L.N., 2000. Anisotropy in the Australasian upper mantle from Love and Rayleigh waveform inversion. *Earth Planet. Sci. Lett.* 184, 339–351.
- Dziewonski, A., Hager, B., O'Connell, R., 1977. Large-scale heterogeneities in the lower mantle. *J. Geophys. Res.* 82, 239–255.
- Farnetani, C.G., Lagras, B., Tackley, P.J., 2002. Mixing and deformations in mantle plumes. *Earth Planet. Sci. Lett.* 196, 1–15.
- Faul, U.H., Jackson, I., 2005. The seismological signature of temperature and grain size variations in the upper mantle. *Earth Planet. Sci. Lett.* 234, 119–134.
- Forte, A., Mitrovica, J., 2001. Deep mantle high-viscosity flow and thermochemical structure inferred from seismic and geodynamic data. *Nature* 410, 1049–1056.
- Foulger, G.R., Pritchard, M.J., Julian, B.R., Evans, J.R., Allen, R.M., Nolet, G., Morgan, W.J., Bergsson, B.H., Erlendsson, P., Jakobsdottir, S., Ragnarsson, S., Stefansson, R., Vogfjord, K., 2000. The seismic anomaly beneath Iceland extends down to the mantle transition zone and no deeper. *Geophys. J. Int.* 142, F1–F5.
- Foulger, G.R., Pritchard, M.J., Julian, B.R., Evans, J.R., Allen, R.M., Nolet, G., Morgan, W.J., Bergsson, B.H., Erlendsson, P., Jakobsdottir, S., Ragnarsson, S., Stefansson, R., Vogfjord, K., 2001. Seismic tomography shows that upwelling beneath Iceland is confined to the upper mantle. *Geophys. J. Int.* 146, 504–530.
- Goes, S., van der Lee, S., 2002. Thermal structure of the north American uppermost mantle inferred from seismic tomography. *J. Geophys. Res.* 107. doi:10.1029/2000JB000049.
- Goes, S., Spakman, W., Bijwaard, H., 1999. A lower mantle source for central European volcanism. *Science* 286, 1928–1931.
- Goes, S., Govers, R., Vacher, P., 2000. Shallow mantle temperatures under Europe from P and S wave tomography. *J. Geophys. Res.* 105, 11153–11169.
- Hung, S.-H., Dahlen, F., Nolet, G., 2000. Frechet kernels for finite-frequency travel times — II. Examples. *Geophys. J. Int.* 141, 175–203.
- Hung, S.H., Shen, Y., Chiao, L.Y., 2004. Imaging seismic velocity structure beneath the Iceland hot spot: a finite frequency approach. *J. Geophys. Res.* 109, B08305. doi:10.1029/2003JB002889.
- Káráson, H., van der Hilst, R.D., 2001. Tomographic imaging of the lowermost mantle with differential times of refracted and diffracted core phases (PKP, P-diff). *J. Geophys. Res.* 106, 6569–6587.
- Karki, B., Wentzcovitch, R., de Gironcoli, S., Baroni, S., 2001. First principles thermoelasticity of MgSiO₃-perovskite: consequences for the inferred properties of the lower mantle. *Geophys. Res. Lett.* 28, 2699–2702.
- Kellogg, L., Hager, B., van der Hilst, R., 1999. Compositional stratification of the deep mantle. *Science* 283, 1881–1884.
- Kiefer, B., Stixrude, L., Wentzcovitch, R., 2002. Elasticity of (Mg,Fe) SiO₃-perovskite at high pressures. *Geophys. Res. Lett.* 29, 1539.
- Komatitsch, D., Tromp, J., 2002a. Spectral-element simulations of global seismic wave propagation — i. Validation. *Geophys. J. Int.* 149, 390–412.
- Komatitsch, D., Tromp, J., 2002b. Spectral-element simulations of global seismic wave propagation — ii. Three-dimensional models, oceans, rotation and self-gravitation. *Geophys. J. Int.* 150, 303–318.
- Korenaga, J., 2003. Energetics of mantle convection and the fate of fossil heat. *Geophys. Res. Lett.* 30. doi:10.1029/2003GL01692.
- Lei, J., Zhao, D., 2006. A new insight into the Hawaiian plume. *Earth Planet. Sci. Lett.* 241, 438–453.
- Li, X.D., Romanowicz, B., 1995. Comparison of global waveform inversions with and without considering cross branch coupling. *Geophys. J. Int.* 121, 695–709.
- Megnin, C., Romanowicz, B., 2000. The three-dimensional shear velocity structure of the mantle from the inversion of body, surface and higher-mode waveforms. *Geophys. J. Int.* 143, 709–728.
- Montelli, R., Nolet, G., Dahlen, F.A., Masters, G., Engdahl, E.R., Hung, S.H., 2004. Finite-frequency tomography reveals a variety of plumes in the mantle. *Science* 303, 338–343.
- Montelli, R., Nolet, G., Dahlen, F., 2006a. Comment on 'banana-doughnut kernels and mantle tomography' by van der Hilst and de Hoop. *Geophys. J. Int.* 167, 1204–1210.
- Montelli, R., Nolet, G., Dahlen, F., Masters, G., 2006b. A catalogue of deep mantle plumes: new results from finite-frequency tomography. *Geochem. Geophys. Geosyst.* (G3). doi:10.1016/j.chemgeo.2007.01.022.
- Morse, S., 2000. A double magmatic heat pump at the core-mantle boundary. *Am. Mineral.* 85, 1589–1594.
- Nakagawa, T., Tackley, P., 2004. Effect of the thermochemical convection on the thermal evolution of the earth's core. *Earth Planet. Sci. Lett.* 220, 107–119.
- Nolet, G., 1990. Partitioned wave-form inversion and 2D structure under the NARS array. *J. Geophys. Res.* 95, 8513–8526.
- Nolet, G., Karato, S.-i., Montelli, R., 2006. Plume fluxes from seismic tomography. *Earth Planet. Sci. Lett.* 248, 685–699.
- Rhodes, M., Davies, J., 2001. Tomographic imaging of multiple mantle plumes in the uppermost lower mantle. *Geophys. J. Int.* 147, 88–92.
- Ritsema, J., Allen, R., 2003. The elusive mantle plume. *Earth Planet. Sci. Lett.* 207, 1–12.
- Ritsema, J., van Heijst, H.J., Woodhouse, J.H., 1999. Complex shear wave velocity structure imaged beneath Africa and Iceland. *Science* 286, 1925–1928.
- Romanowicz, B., Gung, Y., 2002. Superplumes from the core-mantle boundary to the lithosphere: implications for heat flux. *Science* 296, 513–516.
- Sigloch, K., Nolet, G., 2006. Measuring finite-frequency body wave amplitudes and travel times. *Geophys. J. Int.* 167, 271–287.

- Simons, F.J., van der Hilst, R.D., Montagner, J.P., Zielhuis, A., 2002. Multimode Rayleigh wave inversion for heterogeneity and azimuthal anisotropy of the Australian upper mantle. *Geophys. J. Int.* 151, 738–754.
- Sleep, N., 1990. Hotspots and mantle plumes: some phenomenology. *J. Geophys. Res.* 95, 6715–6736.
- Solomatov, V.S., 2001. Grain size-dependent viscosity convection and the thermal evolution of the Earth. *Earth Planet. Sci. Lett.* 191, 203–212.
- Stefansson, R., Bodvarsson, R., Slunga, R., Einarsson, P., Jakobsdottir, S., Bungum, H., Gregersen, S., Havskov, J., Hjelme, J., Korhonen, H., 1993. Earthquake prediction research in the south Iceland seismic zone and the SIL project. *Bull. Seismol. Soc. Am.* 83, 696–716.
- Steinberger, B., 2000. Plumes in a convective mantle: models and observations for individual hotspots. *J. Geophys. Res.* 105, 11127–11152.
- Stixrude, L., Hemley, R., Fei, Y., Mao, H., 1992. Thermoelasticity of silicate perovskite and magnesio-wuestite and stratification of the earth's mantle. *Science* 257, 1099–1101.
- Tarduno, J., Cottrell, R., 1997. Paleomagnetic evidence for motion of the Hawaiian hotspot during formation of the Emperor seamounts. *Earth Planet. Sci. Lett.* 153, 171–180.
- Tromp, J., Tape, C., Liu, Q., 2005. Seismic tomography, adjoint methods, time reversal and banana-doughnut kernels. *Geophys. J. Int.* 160, 195–216.
- van der Hilst, R., de Hoop, M., 2005. Banana-doughnut kernels and mantle tomography. *Geophys. J. Int.* 163, 956–961.
- van der Hilst, R., Karason, H., 1999. Compositional heterogeneity in the bottom 1000 km of the earth's mantle: toward a hybrid convection model. *Science* 283, 1885–1888.
- van der Hilst, R., Engdahl, R., Spakman, W., Nolet, G., 1991. Tomographic imaging of subducted lithosphere below northwest Pacific island arcs. *Nature* 353, 37–43.
- van der Lee, S., Nolet, G., 1997. Upper mantle s velocity structure of north America. *J. Geophys. Res.* 102, 22815–22838.
- Waite, G.P., Smith, R.B., Allen, R.M., 2006. Vp and Vs structure of the Yellowstone Hotspot upper mantle from teleseismic tomography: evidence for an upper-mantle plume. *J. Geophys. Res.* 111. doi:10.1029/2005JB003867.
- Weidner, D., Wang, Y., 1998. Chemical- and Clapeyron-induced buoyancy at the 660 km discontinuity. *J. Geophys. Res.* 103, 7431–7441.
- Wentzcovitch, R., Karki, B., Cococcioni, M., de Gironcoli, S., 2004. Thermoelastic properties of MgSiO₃-perovskite: insights on the nature of the earth's lower mantle. *Phys. Rev. Lett.* 92, 1–4.
- Wolfe, C., Bjarnason, I., VanDecar, J., Solomon, S., 1997. Seismic structure of the Iceland mantle plume. *Nature* 385, 245–247.
- Wolfe, C., Bjarnason, I., VanDecar, J., Solomon, S., 2002. Assessing the depth resolution of tomographic models of upper mantle structure beneath Iceland. *Geophys. Res. Lett.* 29, 1–4.
- Zhao, D., 2001. Seismic structure and origin of hotspots and mantle plumes. *Earth Planet. Sci. Lett.* 192, 251–265.
- Zhao, D., 2004. Global tomographic images of mantle plumes and subducting slabs: insight into deep Earth dynamics. *Phys. Earth Planet. Inter.* 146, 3–34.
- Zhao, D., Hasegawa, A., Horiuchi, S., 1992. Tomographic imaging of P and S wave velocity structure beneath northeastern Japan. *J. Geophys. Res.* 97, 19909–19928.
- Zhao, D., Todo, S., Lei, J., 2005. Local earthquake reflection tomography of the Landers aftershock area. *Earth Planet. Sci. Lett.* 235, 623–631.